MEIJER, C. S. (1946). *Proc. K. Ned. Akad. Wet.* **49**, 227-237, 344-356, 457-469, 632-641, 765-772, 936-943, 1063-1072, 1165-1175.
ROGERS, D. & WILSON, A. J. C. (1953). *Acta Cryst.* **6**, 439-449.
SHMUELI, U., WEISS, G. H. & KIEFER, J. E. (1985). *Acta Cryst.* A**41**, 55-59.
SHMUELI, U., WEISS, G. H., KIEFER, J. E. & WILSON, A. J. C. (1984). *Acta Cryst.* A**40**, 651-660.
WEISS, G. H., SHMUELI, U., KIEFER, J. E. & WILSON, A. J. C. (1985). *Structure and Statistics in Crystallography*, edited by A. J. C. WILSON. Guilderland: Adenine Press.
WILSON, A. J. C. (1949). *Acta Cryst.* **2**, 318-321.
WILSON, A. J. C. (1952). *Research*, **5**, 588-589.

Acta Cryst. (1987). A**43**, 556-564

Maximum Entropy Calculation of Electron Density with Native and Single Isomorphous Replacement Data

BY RICHARD K. BRYAN AND DAVID W. BANNER*

European Molecular Biology Laboratory, Meyerhofstrasse 1, 6900 *Heidelberg, Federal Republic of Germany*

(*Received* 5 *November* 1986; *accepted* 16 *February* 1987)

Abstract

Maximum entropy is applied to the calculation of electron density maps from native and single isomorphous replacement (SIR) intensity data. Native intensity data alone at around 3 Å resolution are shown to be an insufficient constraint to give an interpretable map. When the method is applied to SIR data at the same resolution, either by direct selection between the 'most probable' phases, or by using both intensity data sets directly as constraints, the result is a significant improvement over a conventional 'best' map, as demonstrated by a calculation on data synthesized from a protein fragment. The robustness of the method is demonstrated by a series of calculations using increasingly noisy data.

1. Introduction

Recently, there has been increasing interest in applying maximum entropy in crystallography, ranging from the fundamental theory (Wilkins, Varghese & Lehmann, 1983; Livesey & Skilling, 1985) and the connection with direct methods (Bricogne, 1984) to the presentation of computational results. The latter have shown (*e.g.* Collins, 1982; Bricogne, 1984; Wei, 1985; Wilkins & Stuart, 1986; Navaza, 1986) that if structure factors are supplied to, say, 3 or 4 Å, then structure factor extension is possible (*i.e.* meaningful Fourier coefficients may be generated at reciprocal-lattice points beyond the resolution of the data provided). These calculations are analogous to those of Gull & Daniell (1978), in which the data were Fourier coefficients obtained by radio interferometer observations. However, our opinion is that if reliable multiple isomorphous replacement (MIR) phases are already available to, say, 3 Å resolution, an electron density map produced by direct Fourier synthesis is usually interpretable. Whilst the map quality may be improved by structure factor extension beyond this figure, it is not essential for detailed model building. Delay in many protein structure determinations is frequently due to the difficulty of finding at least two derivatives which are sufficiently isomorphous to the native at 3 Å resolution. Several derivatives might be found which give good data to around 6 Å resolution, but not beyond, either because the crystals diffract poorly, or because the structure is disturbed locally by the inclusion of the heavy atoms so that it becomes non-isomorphous at higher resolution. Many techniques have evolved to make use of partly phased data, such as the use of non-crystallographic symmetry averaging, which has had great success in icosahedral virus structure determination (Harrison, Olson, Schutt, Winkler & Bricogne, 1978; Hogle, Chow & Filman, 1985; Rossmann *et al.*, 1985), where there are a large number of subunit copies in the asymmetric unit. However, such methods cannot be used in the more general problem without symmetry. Another approach has been to combine isomorphous replacement and direct methods (Hauptman, 1982), which, like many established direct methods, requires the assumption of atomicity, and will almost certainly lose power at lower resolution.

In previous work (Bryan, Bansal, Folkhard, Nave & Marvin, 1983), maximum entropy was applied to the calculation of the electron density of the coat protein of the filamentous virus Pfl from fibre diffraction data. Data from the native structure to 4 Å resolution and a single isomorphous derivative to 5 Å resolution were available (Nave *et al.*, 1981). The finite radius of a filamentous structure implies continuity of the structure factors as a function of layer-line radius, which is not ensured if the conventional

* Present address: F. Hoffmann-La Roche, 4002 Basle, Switzerland.

0108-7673/87/040556-09$01.50

crystallographic 'best' phase and figure-of-merit weighting are used point-by-point along a layer line. It is essential to select between the 'most probable' phases in such a way as to give continuous layer lines, and to select correctly between the possible phase choices on different layer lines. This was done by calculating the maximum entropy map which simultaneously fitted both native and derivative data, and it was clearly interpretable as an α-helical structure. The resolution was later successfully extended to 3 Å by the same methods (Marvin, Bryan & Nave, 1987). Here we apply the same technique to crystallographic data with a single isomorphous derivative, and show results for numerical calculations on a small (20 amino acid) protein fragment. The number of possible phase solutions to this problem is potentially much greater than in the equivalent fibre problem, as there is no longer any continuity constraint. We also question the belief that maximizing entropy subject only to native intensity constraints will provide a useful method at resolutions less than atomic. A calculation shows that there is not necessarily an entropy maximum close to the correctly phased solution.

2. Theory

The maximum entropy criterion involves selecting the map which has the greatest configurational entropy (*i.e.* least configurational information) from the 'feasible set' of maps which fit the experimental data to within the noise limits. This technique has been proved to be the unique extremum principle which does not introduce correlations in the map which are not required by the data (Shore & Johnson, 1980; Gull & Skilling, 1984; Livesey & Skilling, 1985). Selection of the map with least configurational information confers many advantages. For example (Gull & Daniell, 1978), there must be evidence in the data for any structure seen in the reconstruction. Noise is automatically suppressed, as are artifacts, such as ringing due to incomplete coverage of reciprocal space by the data.

We start by defining the 'feasible set' of maps as those which are consistent with the observed data. If the differences between the intensities calculated from a given trial map ρ and the observed intensities can be attributed solely to noise on the data, then we claim that our trial map agrees with the data, and is thus a 'feasible' map. If isomorphous replacement or anomalous difference data are also available, then, assuming that the positions of the heavy atoms have already been established, the calculated derivative intensities can similarly be compared with the observations. It is not necessary to go *via* the intermediate step of explicitly calculating the phase probability distribution for each structure factor. The usual comparison measure, already used for many types of data, is the logarithm of the likelihood, giving the χ^2 test (Abels, 1974; Gull & Daniell, 1978). If one assumes uncorrelated noise of known variance, the appropriate form for crystallographic data is

$$\chi^2(\rho; I^n, I^{d_i}, F^p) = \sum_{\mathbf{h}} \Big\{ w^n_{\mathbf{h}}(|F_{\mathbf{h}}|^2 - I^n_{\mathbf{h}})^2 \qquad (1a)$$

$$+ \sum_i w^{d_i}_{\mathbf{h}}(|F_{\mathbf{h}} + H^{d_i}_{\mathbf{h}}|^2 - I^{d_i}_{\mathbf{h}})^2 \qquad (1b)$$

$$+ w^p_{\mathbf{h}}|F_{\mathbf{h}} - F^p_{\mathbf{h}}|^2 \Big\}, \qquad (1c)$$

where $I^n_{\mathbf{h}}$ are the observed native intensities, $I^{d_i}_{\mathbf{h}}$ are the observed intensities for the ith derivative, weighted by $w^n_{\mathbf{h}}$ and $w^{d_i}_{\mathbf{h}}$ (usually inverse variances) respectively, the $F_{\mathbf{h}}$ are the structure factors calculated from a trial map ρ, $H^{d_i}_{\mathbf{h}}$ are the transforms of the heavy-atom contribution to the ith derivative, and the $F^p_{\mathbf{h}}$ phased data, included to take account of reflections which can be phased reliably by conventional isomorphous replacement, such as centrics when a single isomorphous derivative is used.

A statistic comparing the calculated and measured *amplitudes* has also been suggested for the phase problem (Gull & Daniell, 1978; Wilkins *et al.*, 1983). We believe that it is preferable to define the χ^2 test on the intensities (Bryan, 1980, 1984; Bryan *et al.*, 1983; Livesey & Skilling, 1985; Wilkins, Steenstrup & Varghese, 1985), as it gives a constraint function which is differentiable everywhere, including the origin, in each complex plane, and is also a more natural definition since the measured data are the intensities. The amplitude statistic is non-differentiable if any amplitude is zero, so it would be impossible to start the iterative algorithm from a flat map, which may be desirable if the phases are not to be biased to those of a particular model starting map. However, the reconstructions obtained are unlikely to be significantly different if the signal-to-noise ratio is reasonably high, as they give the same form for small deviations around the position of exact fit.

The form of constraint function we use can be extended to include data from further derivatives, simply by adding extra terms like (1*b*). Anomalous differences can be incorporated most easily by treating the $I^{(+)}$ and $I^{(-)}$ measurements separately, each being compared with the appropriate structure factor plus heavy atom contribution. If the measurements of the Bijvoet pair are given equal weights, it is also possible to rearrange the equations to give a comparison on the average intensity plus a further contribution on the anomalous difference itself, so that $|F+H|^2+|H''|^2$ is compared with I^{av}, and $4\,\text{Im}\,[(F+H)H''^*]$ with ΔI^{anom}. Here H is the structure factor calculated from the sum of the normal and the real part of the anomalous scattering factors of the heavy atoms, and H'' the corresponding quantity for the imaginary component of the anomalous scattering factors. This form enables the effect of the

anomalous differences to be assessed directly, but it is important to note that the natural data are the average intensities and the intensity anomalous differences, rather than the corresponding quantities defined on amplitudes, as is the usual practice.

As in any form of statistical testing, the χ^2 test enables one to determine whether a trial map ρ is an acceptable fit to the data at a given confidence level. If one assumes that the central limit theorem can be applied to the noise distribution (which will include Gaussian and Poisson noise), and that the total number M of intensity measurements is large, the distribution of the χ^2 statistic can be approximated by an $\mathcal{N}(M, 2M)$ Gaussian, and so a trial map ρ which gives a $\chi^2 \geq M + 3{\cdot}3\sqrt{M}$ can be rejected as incompatible with the data at 99% confidence; thus the feasible set is those maps that gave a χ^2 value less than this. The member of this set having the greatest configurational entropy S, where

$$S(\rho) = -\sum_j p_j \log p_j/m_j, \quad p_j = \rho_j/\sum \rho, \qquad (2)$$

is selected as the maximum entropy solution. **m** is the normalized prior map, which is the estimate of the solution before the data are considered, and $\mathbf{p} = \mathbf{m}$ has the global unconstrained entropy maximum. If **m** lies within the feasible set, it will be the maximum entropy solution, which should only happen if the data introduce no new information. Usually, **m** is taken as the completely unbiased flat map, which will only lie within the feasible set if the data are so noisy that they convey no information whatsoever. Otherwise, since the entropy function is convex, any feasible maximum entropy map will lie on the surface of the feasible set.

If constraint (1c) alone is used, the map and data are linearly related, the feasible set of maps defined by the χ^2 test is an ellipsoidal cylinder in the space of all maps, and there is a unique entropy maximum. The topology of the feasible set if intensity constraints are also used is, however, more complicated. Exact knowledge of an intensity constrains the corresponding structure factor to lie on a circle in the complex plane, which will be blurred into an annulus by noise on the data. If native and derivative intensity constraints are used, there may be disconnected regions of high likelihood, which when projected in the amplitude direction give the classical bimodal phase probability distribution. Fig. 1(a) shows a contour map of the contribution to the likelihood, $\exp(-\frac{1}{2}\chi^2)$, for one reflection with data on the intensities of the native and a single isomorphous derivative, stemming from the example in § 4. If, however, there is little phase information for a reflection in the SIR data, the χ^2 distribution will remain more nearly circularly symmetric (Fig. 1b). Thus, depending on the data, a given structure factor may be constrained to lie within an annulus or in one or two simply connected regions of the complex plane, or be completely unconstrained. The feasible set, if data are provided for M reflections, is the M-dimensional product of such regions, extending to infinity in those directions for which there are no data. Use of the entropy function, which automatically restricts maps to the positive orthant $\rho_j \geq 0$, may eliminate many of the disconnected regions, but may also introduce extra topological complications if the orthant edges intersect parts of the feasible set. We may thus expect to find several local entropy maxima when intensity constraints are used, corresponding to the possible phase ambiguities of the problem. Unfortunately, the global optimization problem is not yet solved, and we are unable to explore enough of the N-dimensional space of maps to discover all the local maxima, and thus be able to choose the global maximum. What we can do is to construct an iterative algorithm which is

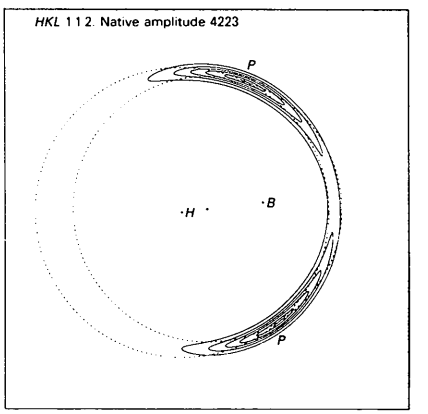

(a)

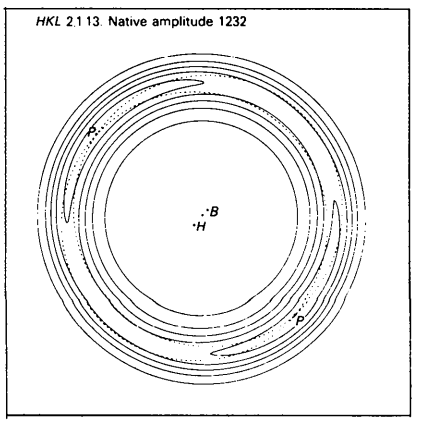

(b)

Fig. 1. Contour maps in the complex plane of likelihood contribution, $\exp(-\frac{1}{2}\chi^2)$, for single reflections. H denotes the heavy atom contribution, B the 'best' structure factor, and P the 'most probable' structure factors, where the native and derivatives amplitudes (dotted circles) intersect in a Harker construction. Contour levels are 0·1, 0·3, 0·5, 0·7, 0·9. The native amplitudes have been normalized to the same size. (a) Bimodal phase distribution. (b) Phase not well defined.

sufficiently robust to have a good chance of reaching some local entropy maximum without becoming trapped. Which of the possible maxima (assuming that there is more than one) is reached will depend on the starting map.

The numerical algorithm we have used to solve the problems described in §§ 3 and 4 has been described in detail in Skilling & Bryan (1984) for the case of convex constraints, and the extension to non-convex constraints in Bryan & Skilling (1986). Despite criticisms of this algorithm (Bricogne, 1984), there is no difficulty in employing it to find local maxima of the non-convex constrained problem. Indeed, the original motivation for the development of this algorithm (Bryan, 1980) was the phase problem in the context of radio astronomy, and it has been used for the solution of the SIR fibre diffraction problem (Bryan *et al.*, 1983; Marvin *et al.*, 1987). A global solution to the problem is much harder. One approach might be to construct a scheme to examine systematically all the possible local maxima, as has been suggested by Bricogne (1984).

3. Native intensity data

The ideal method for electron-density calculations would be 'direct', using only native intensity data, but the numerical solution of this problem is fraught with the possibilities of multiple local maxima, and an *ab initio* calculation would inevitably be extremely computer intensive. Moreover, practical calculations performed previously (Bryan, 1984) indicated that the correctly phased solution is not necessarily at or near *any* local entropy maximum. We illustrate this here with an example using data for the 'blue protein' from *Alcaligenes faecalis*, whose structure has been solved in this laboratory (Petratos, Banner, Tsernoglou & Beppu, 1987), using SIR plus anomalous differences. This protein has a molecular weight of 12 000, and crystallizes in space group $P6_5$, $a = b = 50$, $c = 98{\cdot}5$ Å, with one molecule per asymmetric unit.

A maximum entropy map was calculated using the experimentally derived structure factors to 2·9 Å resolution (average FOM 80%) as a constraint of type (1*c*). An atomic model had already been built into this density, indicating that the phases must have been reasonably close to the 'true' phases. Qualitatively the maximum entropy map (Fig. 2*a*) was very similar to the usual 'best' map, but with the density standing out with greater contrast against a more uniform background. This calculation was equivalent to those cited in § 1.

A second maximum-entropy map was calculated, using the first as the starting map, but now ignoring the experimental phases by using only native intensities in the constraint function (1*a*). We would expect that if there were a local maximum of entropy for this problem close to the map produced using the constraint with phases, it would be found by this computation. However, the resulting map (Fig. 2*b*) had an average amplitude-weighted phase change,

$$\sum_{\mathbf{h}} |F_{\mathbf{h}}| |\varphi_{\mathbf{h}}^{me} - \varphi_{\mathbf{h}}^{ir}| \Big/ \sum_{\mathbf{h}} |F_{\mathbf{h}}|, \qquad (3)$$

of 37·6° from the original phases, and the entropy had risen from −1·6749 to −0·8817. The density itself had become rather broken, and chain-tracing was no longer possible. Although only a single counter-example, it casts doubt on whether an interpretable density can be derived in general from native intensity data only at this resolution. Navaza (1986) has also noted that a maximum-entropy map constrained by native intensities only was uninterpretable in terms of molecular structures, although he does not define the starting map for his calculation.

Jaynes (1968, 1982) points out that if the entropy of an observed distribution is significantly less (in a sense that he makes precise) than that of the

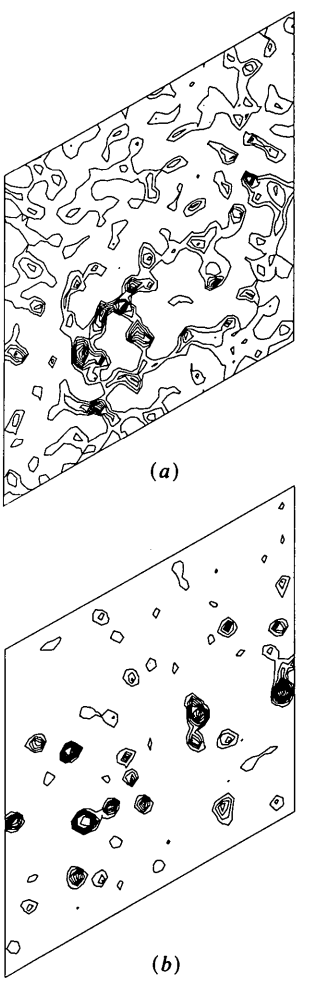

Fig. 2. Single sections of blue protein density from (*a*) IR structure factors and maximum entropy, (*b*) native intensities, starting from map (*A*). Contour levels are the same in both plots, at 10, 20%, ... of the overall maximum.

maximum entropy distribution calculated according to a given hypothesis, then there is evidence that systematic influences, other than those incorporated into the hypothesis, are constraining the observed system. Let us take as the 'observed distribution' the maximum entropy density found using the experimental structure factors. This density must have a greater entropy than that of the 'true' density, as, say, using additional higher-resolution data will add constraints to the system, and thus reduce the entropy, or possibly leave it unchanged if the new constraints are redundant. For the theoretical distribution, we take the density produced using native intensity data; our hypothesis is effectively that intensity constraints are sufficient for us to deduce all the structure in the system at this resolution, and that the phases contain no additional information. The entropy values calculated above convincingly demonstrate otherwise. Indeed, we already believe strongly from other evidence, but are unable to deduce directly from the diffraction data to hand, that the structure is made of atoms, arranged into molecules with specific stereochemistry, causing systematic departures from the uniform density that is assumed for the prior in this application of maximum entropy. It is this belief that would inevitably cause a map such as Fig. 2(*b*) to be rejected as a possible solution for the crystal structure.

Ideally, our method of solution should give only densities which could be produced by atomic structures with correct stereochemistry. Information such as allowable bond lengths and angles, and, at a larger scale, of secondary and tertiary structures, should be used if possible. Although the entropy expression (2) provides a way of incorporating prior information *via* **m**, direct modification of **m** would imply that the absolute positions of the features were known, and hence also the phases. However, our stereochemical information is really in terms of spatial correlation of density, and not the density itself. Some preliminary work to incorporate density correlations into a prior map has been performed (Skilling, 1986; Bryan, 1986), but it has not yet reached the stage when it can encode information at the complexity of molecular structures. Therefore, given these considerations, and the numerical results described above, we consider that the *ab initio* problem using only native intensity constraints at around 3 Å resolution is perhaps not the most useful one to approach at present.

An alternative way of introducing further constraints is of course to use more data pertaining to the phases. In the limiting case these would be the MIR phases, and the problem will have a unique solution. Here, we approach an intermediate problem, the use of single isomorphous replacement data, and investigate whether the use of maximum entropy is an improvement over straightforward Fourier methods.

4. Single isomorphous replacement data

Whilst in some circumstances a conventional figure-of-merit weighted SIR Fourier map (Blow & Rossmann, 1961) may be interpretable, this is not always the case. In general, SIR data give a choice of two possible phases for each structure factor, the two 'most probable' phases. The classical way of using such data is to compute the 'best' map, which is a Fourier synthesis from the average of the two possible structure factors. Thus neither the phases nor the amplitudes of the computed map are correct. This map is 'best' only in the sense that it minimizes the sum of the squared differences from both the possible phase solutions. Instead, we shall attempt to select between the possible 'most probable' phases, so that our map will at least agree with the data. The number of acceptable 'most probable' maps will be considerably reduced by positivity alone, although it will probably not resolve the ambiguity in phase of weaker reflections in particular, where an incorrect phase choice would not cause this criterion to be violated.

We have investigated two approaches to this problem: firstly, an attempt to solve the finite (although very large!) problem of finding which of the 2^M possible phase solutions maximizes the entropy, and, secondly, the use of native and derivative data directly in the χ^2 statistic as defined above.

Method 1. For each reflection, the two 'most probable' phases were calculated and one chosen arbitrarily. With this set of structure factors as a phased data constraint (1*c*), a maximum entropy map was calculated. The entropy was naturally very low, since a random selection of 'most probable' phases will not in general give a positive structure, and consequently many points had densities approaching zero. The residuals, $\sqrt{w}|F^{me} - F^{p}|$, for each structure factor were examined, where F^p now represents the current choice of 'most probable' structure factor. If the residual was greater than the residual would have been for the other phase choice, the structure factor in the data set was replaced by the other choice. Such a procedure must lead to a map with a larger entropy when the fit to the data is equally good. Next, the structure factor with the largest residual was exchanged for the other phase choice, and a new maximum entropy map calculated. If this showed an increase in entropy compared with the previous map, another reflection was similarly exchanged. Otherwise, it was changed back, the one with the next-largest residual tried, and the process repeated iteratively. Clearly, with a large number of reflections, this process might be extremely lengthy. The effect is to examine a subset of all the possible phase solutions in a controlled way. The advantage of this method lies in the convexity of the constraint function for each particular choice of phases, so that each individual maximization problem has a unique sol-

. ution, and a fast and reliable numerical algorithm can be used. Nevertheless, because of the many subproblems that must be solved, the total computer time required turns out to be comparable to method (2). A further disadvantage is that the error model is isotropic (*i.e.* the variances in the amplitude and phase directions are equal), which is also the case for Wilkins & Stuart (1986). Their estimate of variance depends on the reliability of the phase, but is then applied isotropically. Thus information in accurately known amplitudes may be lost because the phasing is inaccurate.

Method 2. The native and derivative data sets were used together as constraints - the intensities of the transform of the trial electron density were compared with the native data, and the intensities of the map transform plus heavy-atom contribution with the derivative data set, using terms (1*a*) and (1*b*) in χ^2, as was done for the SIR fibre problem (Bryan *et al.*, 1983). For a given reflection, the net effect is to give a good fit to the data only if the calculated structure factor is near either of the classical 'most probable' values, as discussed in § 2. Since this problem exhibits the full complexity of optimization with non-convex constraints, it takes much more computer time to solve than a similar-sized convex problem. The single derivative is sufficient to phase the centrosymmetric reflections, which are therefore incorporated in the phased term (1*c*), except that those with a low figure of merit, below 0·75, are ignored.

We describe here a calculation using simulated data. We obtained a representative piece of protein by extracting a fragment of 20 amino acids (160 non-hydrogen atoms) forming an α-β motif from triose phosphate isomerase (Banner, Bloomer, Petsko, Phillips & Wilson, 1976), placed it in the asymmetric unit of a $P2_12_12_1$ unit cell, $a=b=24$, $c=64$ Å, and calculated the structure factors to 3 Å resolution. Part of the density synthesized from these structure factors is shown in Fig. 3. A derivative data set was simulated by adding the structure factors of a single zinc atom per asymmetric unit to the native structure factors, giving a heavy-atom contribution of about the same size as that expected from a real heavy atom in a medium-sized protein, *e.g.* one mercury atom in a protein of molecular weight 16 000, using the formula of Crick & Magdoff (1956). The data used in the following calculations were the intensities of these two sets of structure factors. The heavy-atom parameters were refined in order to emulate the real situation where these parameters are estimated initially from a difference Patterson map. A conventional SIR 'best map' synthesized from these data is shown in Fig. 4 (map *A*). The average figure of merit for all reflections, including centrics, was 68%, and for the acentrics the average amplitude-weighted phase difference between the original simulated phases and the 'best' phases was 43°. Use of these 'best' SIR structure factors as a constraint in a maximum entropy calculation would be inappropriate; they do not necessarily correspond to a positive structure.

Application of the two algorithms described above gave the results displayed in Figs. 5 and 6 (maps *B* and *C*). The heavy atom structure factors used were the same as in the SIR synthesis. Table 1 describes

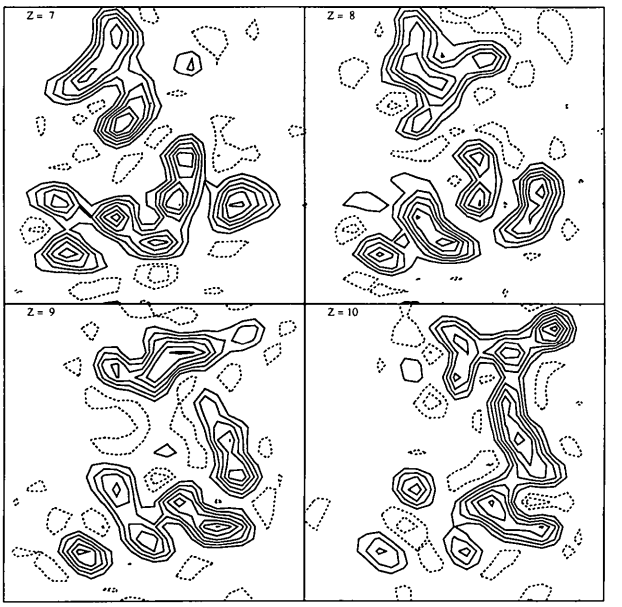

Fig. 3. Density calculated from model protein fragment. Contour map of four successive sections at 1 Å intervals in *z*. This, and all subsequent contour maps, have the same contour intervals. The zero contour is suppressed, and negative contours dashed.

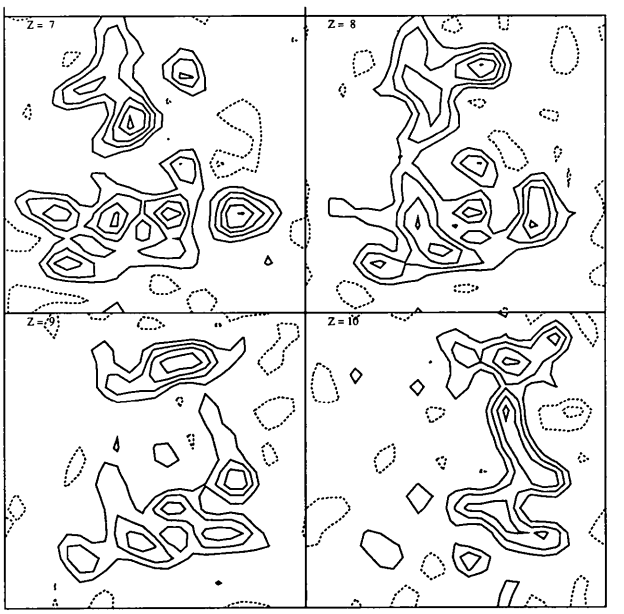

Fig. 4. Density from SIR data by classical 'best' method (map *A*).

Table 1. *Phase changes of acentric reflections resulting from the various calculations described in* § 4

The entropy values (where appropriate) and average amplitude phase change in degrees [equation (3)] from the synthesized native structure factors are given, both overall, and in equal $[(\sin\theta)/\lambda]^2$ ranges. The columns refer to the maps as follows: *A* FOM weighted Fourier synthesis; *B* method 1; *C*–*H* method 2; *C* start flat; *D* start *A* with negatives deleted; *E* start *B*; *F* as *C*, but 5% noise; *G* as *F*, but 20% noise; *H* as *F*, but 40% noise.

			A	*B*	*C*	*D*	*E*	*F*	*G*	*H*
S			—	−8·215	−6·667	−6·668	−6·903	−6·620	−5·623	−3·791
Amplitude weighted phase change (°)										
Average			42·98	20·00	8·51	8·67	11·80	9·31	13·27	35·56
In resolution range		Number of reflections								
∞	11·18	4	60·12	1·15	4·45	4·62	2·09	2·83	9·29	12·99
11·18	7·91	15	39·26	4·77	3·26	3·42	4·18	3·23	3·80	20·83
7·91	6·45	24	35·49	7·13	3·56	3·70	4·15	3·61	4·56	19·79
6·45	5·59	26	40·56	8·47	3·69	3·54	4·63	3·95	5·22	30·67
5·59	5·00	34	46·93	7·62	3·96	3·93	5·06	4·22	6·59	28·68
5·00	4·56	39	45·33	17·26	4·88	4·89	6·58	5·20	7·33	35·68
4·56	4·23	40	41·73	14·65	5·63	5·56	8·74	6·52	8·86	32·47
4·23	3·95	43	33·60	12·66	8·61	8·74	9·32	9·42	14·43	36·88
3·95	3·73	54	41·88	22·92	9·44	10·58	10·16	11·21	13·79	40·53
3·73	3·54	58	40·63	28·59	10·80	10·84	15·64	11·18	14·09	41·16
3·54	3·37	48	42·47	31·60	9·85	9·78	20·45	9·99	14·56	35·95
3·37	3·23	64	47·84	27·75	10·37	10·44	15·86	11·68	16·85	36·84
3·23	3·10	57	50·65	30·27	15·19	15·56	20·64	17·88	28·50	49·23
3·10	3·00	53	47·38	36·93	17·60	17·63	24·01	18·47	27·41	43·58

the phase differences from the simulated structure factors. The average phase error increases with resolution, but this could be expected, as it gives about the same positional accuracy at all resolutions.

There is a practical limit to the first method; eventually the distribution of residuals agrees with the expected distribution, and it is no longer possible to distinguish outliers as candidates for phase exchange, *i.e.* it is just as likely that a large residual is due to a genuine bad fit to a correctly phased datum as to one incorrectly phased. About a quarter of the total number of reflections, mostly small and medium sized, remained at the incorrect phase choice. Since all reflections contribute with full amplitude, these have a fairly adverse affect on the map, leading to significant artifacts, whereas in conventional figure-of-merit weighted maps the imprecisely phased reflections are reduced in amplitude. Furthermore, since the heavy atom model had been refined, and thus some heavy atom structure factors differed significantly from the true ones, some reflections were badly phased - neither 'most probable' phase was

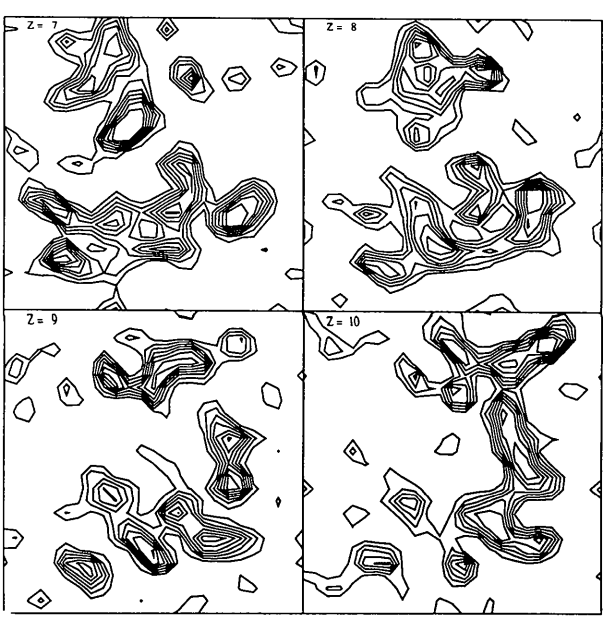

Fig. 5. Density from SIR data by method 1 (map *B*).

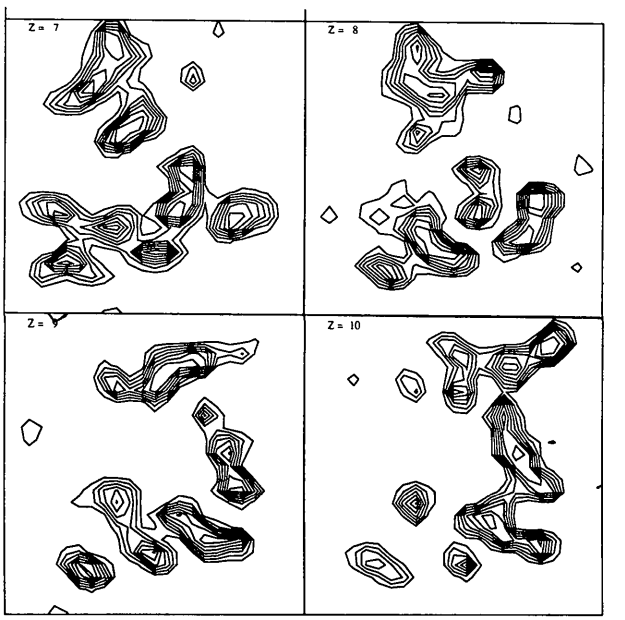

Fig. 6. Density from SIR data by method 2 (map *C*).

near the true one. Even in a conventional SIR synthesis, the figure of merit of such reflections may be large. Phases of reflections which were imprecisely phased, perhaps because of a small heavy atom contribution, may also be far from their true values, yet the constraint is as strong as for well phased reflections.

The second method, with a better probabilistic model of the errors in the data, does not suffer from this disadvantage. If the phase determination is imprecise, the constraint is effective on amplitude only. If precise, then good fits to the data will be found only near the classical 'most probable' phases. The result is a map showing all the correct features and no artifacts, and indeed, owing to the constraint of positivity, shows a sharper structure than the original 3 Å Fourier synthesis, because of a reduction in series termination effects. Since the average amplitude weighted phase change from the original calculated structure factors was only 8·5°, it is clear that the phasing is considerably improved over the conventional 'best' map, and that most of the strong reflections must be correctly phased.

The main disadvantage is that uniqueness of the solution is not ensured. Without a multisolution algorithm, not all local maxima can necessarily be explored. However, we have used several different starting densities, including the flat map, a conventional SIR map with negatives deleted, and the map resulting from method 1, and the resulting densities (maps *C*, *D*, *E*, Table 1) were visually essentially identical, although differing in the exact phasing of weak reflections. The largest average amplitude weighted phase change from the original calculated structure factors obtained was less than 12°. An examination of all possible local entropy maxima would not change the structural interpretation of the map.

Perhaps an optimal scheme would be to use the two methods successively, since the first can, in comparatively few iterations, produce a map whose transform has most of the stronger reflections correctly phased. The resultant map may be used (i) either directly as a starting map, or (ii) as a prior map **m**, in further refinement by method (2). The first method could also be developed further, perhaps by changing the phasing of groups of reflections simultaneously, rather than singly, and thus be speeded up considerably.

The above calculations were all performed using noise-free data, although the value of χ^2 required was appropriate for a noise level of about 1% of the average amplitude. To test the robustness with respect to noise, the calculation using method (2) was repeated, but with Gaussian random noise of standard deviation 5% of the average amplitude added to the simulated amplitudes (giving a variance on the intensities roughly proportional to the intensity; a few of the largest amplitudes reach about ten times the average). Two different starting maps were used: the flat map, and the map produced by the original calculation. The resulting maps were virtually identical, and very similar to the map calculated from noise-free data, although displaying a slight drop in sharpness and an increase in entropy (*F*, Table 1), as would be expected. Increasing the noise successively to 20 and 40% accentuated these effects, with phase errors increasing (*G* and *H*, Table 1) and features beginning to fade out, but still with low noise in the final map (Fig. 7). Eventually, with noise of 150% of the average amplitude, the χ^2 for the flat map becomes less than *M*, the number of observations, showing that no information can be extracted from these data by *using the* χ^2 *test*, despite the fact that the largest intensities are still at the 4–5 standard deviation level.

The constraint functions we have introduced can clearly be used with any number and quality of derivative data sets. If some reflections are judged to be reliably phased by conventional MIR phasing, perhaps low resolution ones if there are several derivatives good to low resolution, the MIR phase can be used to give a structure factor constraint (1*c*). It is a waste of computer time to put in all the intensity data as constraints (1*a*) and (1*b*) in this case. Less reliably phased reflections can still be constrained by the intensities of the native and whatever derivatives provide data. The heavy atom parameters can also be refined at any stage, simply by minimizing χ^2 with respect to them, keeping the current protein structure factors fixed, as was done for the Pf1 refinement. Derivative scale factors can be refined similarly, to give a closed form solution since χ^2 is quadratic in the scale factors. We foresee no difficulty, apart from

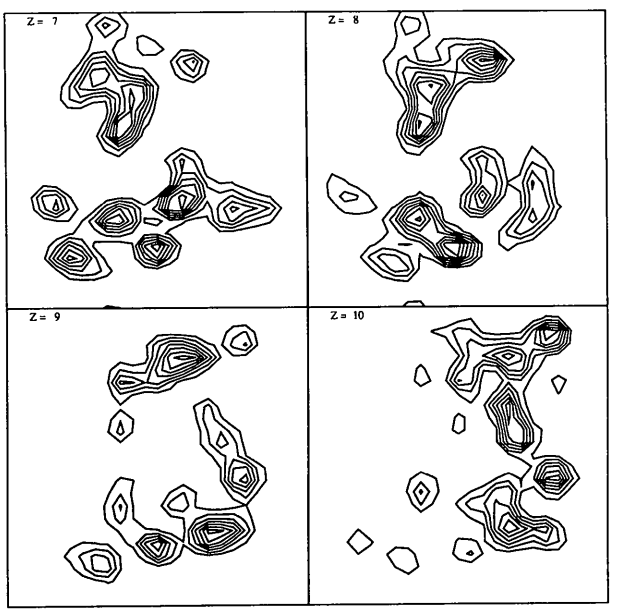

Fig. 7. Density from SIR data with added noise of 40% of average amplitude, by method 2 (map *H*).

greater computational time, in applying this method to larger structures than illustrated here.

References

ABELS, J. G. (1974). *Astron. Astrophys. Suppl.* **15**, 383-393.

BANNER, D. W., BLOOMER, A. C., PETSKO, G. A., PHILLIPS, D. C. & WILSON, I. A. (1976). *Biochem. Biophys. Res. Commun.* **72**, 146-155.

BLOW, D. M. & ROSSMANN, M. G. (1961). *Acta Cryst.* **14**, 1195-1202. Correction: *Acta Cryst.* (1962), **15**, 1060.

BRICOGNE, G. (1984). *Acta Cryst.* A**40**, 410-445.

BRYAN, R. K. (1980). *Maximum Entropy Image Processing.* PhD Thesis, Univ. of Cambridge.

BRYAN, R. K. (1984). Paper presented at the EMBO Workshop on Maximum Entropy Methods in the X-ray Phase Problem, Orsay, France, 24-28 April.

BRYAN, R. K. (1986). Paper presented at the Sixth Workshop on Maximum Entropy and Bayesian Methods in Applied Statistics, Univ. of Seattle, WA, 5-8 August. (Proceedings to be published by Cambridge Univ. Press.)

BRYAN, R. K., BANSAL, M., FOLKHARD, W., NAVE, C. & MARVIN, D. A. (1983). *Proc. Natl Acad. Sci. USA*, **80**, 4728-4731.

BRYAN, R. K. & SKILLING, J. (1986). *Opt. Acta*, **33**, 287-299.

COLLINS, D. M. (1982). *Nature (London)*, **254**, 49-51.

CRICK, F. H. C. & MAGDOFF, B. S. (1956). *Acta Cryst.* **9**, 901-908.

GULL, S. F. & DANIELL, G. J. (1978). *Nature (London)*, **272**, 686-690.

GULL, S. F. & SKILLING, J. (1984). In *Indirect Imaging*, edited by J. A. ROBERTS, pp. 267-279. Cambridge Univ. Press.

HARRISON, S. C., OLSON, A. J., SCHUTT, C. E., WINKLER, F. K. & BRICOGNE, G. (1978). *Nature (London)*, **276**, 368-373.

HAUPTMAN, H. (1982). *Acta Cryst.* A**38**, 289-294.

HOGLE, J. M., CHOW, M. & FILMAN, D. J. (1985). *Science*, **229**, 1358-1365.

JAYNES, E. T. (1968). *IEEE Trans. Syst. Sci. Cybern.* **4**, 227-241.

JAYNES, E. T. (1982). *Proc. IEEE*, **70**, 939-952.

LIVESEY, A. K. & SKILLING, J. (1985). *Acta Cryst.* A**41**, 113-122.

MARVIN, D. A., BRYAN, R. K. & NAVE, C. (1987). *J. Mol. Biol.* **193**, 315-343.

NAVAZA, J. (1986). *Acta Cryst.* A**42**, 212-223.

NAVE, C., BROWN, R. S., FOWLER, A. G., LADNER, J. E., MARVIN, D. A., PROVENCHER, S. W., TSUGITA, A., ARMSTRONG, J. & PERHAM, R. N. (1981). *J. Mol. Biol.* **149**, 675-707.

PETRATOS, K., BANNER, D. W., TSERNOGLOU, D. & BEPPU, T. (1987). In preparation.

ROSSMANN, M. G., ARNOLD, A., ERICKSON, J. W., FRANKENBERGER, E. A., GRIFFITH, J. P., HECHT, H.-J., JOHNSON, J. E., KAMER, G., LUO, M., MOSSER, A. G., RUECKERT, R. R., SHERRY, B. & VRIEND, G. (1985). *Nature (London)*, **317**, 145-153.

SHORE, J. E. & JOHNSON, R. W. (1980). *IEEE Trans. Inf. Theory*, **26**, 26-37. Comments and corrections: *IEEE Trans. Inf. Theory* (1983), **29**, 942-943.

SKILLING, J. (1986). In *Maximum Entropy and Bayesian Methods in Applied Statistics. Proceedings of the Fourth Maximum Entropy Workshop, University of Calgary*, 1984, edited by J. H. JUSTICE, pp. 156-178. Cambridge Univ. Press.

SKILLING, J. & BRYAN, R. K. (1984). *Mon. Not. R. Astron. Soc.* **211**, 111-124.

WEI, W. (1985). *J. Appl. Cryst.* **18**, 442-445.

WILKINS, S. W., STEENSTRUP, S. & VARGHESE, J. N. (1985). In *Structure and Statistics in Crystallography*, edited by A. J. C. WILSON, pp. 113-124. New York: Adenine Press.

WILKINS, S. W. & STUART, D. (1986). *Acta Cryst.* A**42**, 197-202.

WILKINS, S. W., VARGHESE, J. N. & LEHMANN, M. S. (1983). *Acta Cryst.* A**39**, 49-60.

Acta Cryst. (1987). A**43**, 564-568

The Derivation of Twin Laws for (Pseudo-)Merohedry by Coset Decomposition

BY H. D. FLACK

Laboratoire de Cristallographie aux Rayons X, Université de Genève, 24 quai Ernest Ansermet, CH-1211 Genève 4, Switzerland

(*Received* 8 *September* 1986; *accepted* 23 *February* 1987)

Abstract

The generation of possible twin laws for (pseudo-)merohedry by left coset decomposition of the point symmetry of the crystal lattice (metric symmetry) with respect to the crystal point group is presented. Two algorithms for the generation of the system of representatives have been devised. The first produces twin laws in the form of pure rotations of 180° wherever possible, and the second associates operations in pairs related by a centre of symmetry for crystals lacking an inversion centre. The metric symmetry should be determined by means of cell reduction from the measured cell dimensions and the crystal point group derived from the assumed space group. The automatic generation of twinning operations by this algorithm greatly facilitates the testing of twinning and orientation ambiguities by way of least-squares refinement of the twin fractions.

Introduction

Twinning by (pseudo-)merohedry results in the exact superposition of the reciprocal lattices of the twin components and hence leads to the modification of the intensities of Bragg reflections. The automatic treatment of (pseudo-)merohedry should hence be an essential component of any modern computer system undertaking structure solution and refinement. Even for the treatment of untwinned single crystals, a knowledge of the possible twin laws by (pseudo-)merohedry can be crucial, as these represent the alternative orientations of the crystal structure with respect to its own lattice.

0108-7673/87/040564-05$01.50